Cooperative effects of Jahn-Teller distortion, magnetism, and Hund's coupling in the insulating phase of $BaCrO_3$

Gianluca Giovannetti,[1] Markus Aichhorn,[2] and Massimo Capone[1]

[1]*CNR-IOM-Democritos National Simulation Centre and International School for Advanced Studies (SISSA), Via Bonomea 265, I-34136, Trieste, Italy*

[2]*Institute of Theoretical and Computational Physics, TU Graz, Petersgasse 16, Graz, Austria*

(Received 12 February 2014; revised manuscript received 30 September 2014; published 22 December 2014)

We employ a combination of density functional theory and dynamical mean-field theory to investigate the electronic structure of the recently synthesized insulator $BaCrO_3$. Our calculations show that Hund's coupling is responsible for strong correlation effects, which are however not sufficient to turn the system insulating without breaking any symmetry. The Hund's correlated metal is however unstable with respect to orbital ordering, which indeed makes the system insulating. The orbitally ordered insulator favors Jahn-Teller distortions and a secondary magnetic ordering.

DOI: 10.1103/PhysRevB.90.245134 PACS number(s): 71.27.+a, 71.10.Fd, 71.30.+h, 75.25.Dk

I. INTRODUCTION

Strongly correlated materials are characterized by narrow valence bands arising from localized atomic orbitals. The reduced itinerancy of the carriers is the gateway that leads to the remarkable variety of phases and regimes observed in d- and f-electron systems. Usually strong electronic correlations are associated with the proximity of a Mott insulating state when the screened local Coulomb interaction U reaches a critical value U_c comparable with the bandwidth W of the system. For pure Hubbard-like interactions U_c would increase with the orbital degeneracy. However, in a multiorbital system, the Hund's exchange does not simply lead to a multiplet splitting, but it qualitatively affects the strength and the nature of the electronic correlations [1]. If the number of the electrons per correlated atoms is an integer, but it is not equal to the number of orbitals (i.e., we are not at half filling), the Hund's coupling increases U_c, but at the same time reduces the coherence of the system at intermediate interactions. This leads to a wide range of interaction parameters where the carriers are strongly correlated, but at the same time far from a Mott insulating state. This novel correlated regime is often referred to as a Hund's metal.

While fingerprints of Hund's metal physics have been reported to explain the bad metallic behavior of iron-based superconductors [2] and ruthenates [3], the interplay of Hund's correlations with electron-lattice coupling and the relationship with magnetic ordering have not been studied in detail. These effects are indeed strongly intertwined. For example, lattice distortions can lead to crystal-field splitting, which lifts the orbital degeneracy and may lead to orbital selective physics [4,5]. In addition, as we will show below, crystal-field splitting can compete with Hund's coupling and Hund's metallicity, since it can induce orbital polarization, whereas Hund's coupling tends to distribute the electrons uniformly in the various orbitals. Furthermore, strong correlation physics is usually associated to the formation of local magnetic moments. The localized spins can typically order in magnetic patterns possibly leading to insulating behavior depending on the interactions and the lattice structure.

The perovskite compounds $ACrO_3$ (A being Ca, Sr, Ba) are a good playground to study this interplay. In those systems Cr has a nominal valence of 4+, with two electrons in the threefold degenerate t_{2g} orbitals. Interestingly, such an electronic configuration is common to both metallic systems like (Ca,Sr)RuO_3 and insulating vanadates with formula RVO_3 (R being rare-earth), in which different orbital and spin orderings establish as a function of temperature [6]. Recently resistance measurements revealed $BaCrO_3$ to be insulating over a large range of temperature with a low-temperature gap of 0.38 eV [7], while there are conflicting evidences of metallic and insulator behaviors in $CaCrO_3$ and $SrCrO_3$ [8–11], and the general question of whether these compounds are metals or insulators is still under debate.

The compound with the smallest A-site ion in the series, $CaCrO_3$, shows an orthorhombically distorted $GdFeO_3$ structure in which the three Cr-O distances are comparable to those found in YVO_3 at room temperature [8] and is characterized by a C-type antiferromagnetic (AFM) magnetic structure [11]. The same C-type magnetism has been reported in $SrCrO_3$ in which however the octahedrallike $GdFeO_3$ distortions are suppressed [11]. Density-functional theory (DFT) calculations, including interaction effects within a DFT+U scheme, found $CaCrO_3$ [12] and $SrCrO_3$ [13] to be either weakly metallic or with a small gap, exhibiting C-type antiferromagnetism with orbital ordering.

To properly account for the delicate balance between inherent correlation effects and the tendency towards ordering, we use a combined approach based on DFT [14] and dynamical mean-field theory (DMFT) [15] which accurately treats the electronic correlations. Our study accounts for the insulating state of $BaCrO_3$, highlighting the role of Coulomb interactions U and J and their interplay with the lattice distortions.

The paper is organized as follows: Section II introduces our methodology, while in Sec. III we turn to describe the results. The section is divided into four subsections devoted respectively to the correlated metallic state in the absence of symmetry breaking, the orbital ordering, the Jahn-Teller distortions, and the magnetic instability. Section IV presents our concluding remarks.

II. METHODS

We start our investigation with DFT calculations within the generalized gradient approximation (using the Perdew-Burke-Ernzerhof (PBE) functional [16]) for the tetragonal unit

cell of $BaCrO_3$ using QUANTUM ESPRESSO [17] and WIEN2K [18] packages. We build Wannier orbitals [19,20] for the t_{2g} (xy,xz,yz) manifold of Cr, which define the basis where we consider the interaction effects. The Coulomb interaction within the t_{2g} manifold is taken in the Kanamori form

$$H_{\rm int} = U \sum_{i,m} n_{im\sigma} n_{im\sigma'} + U' \sum_{i,m,m'} n_{im\sigma} n_{im'\sigma'} + U'' \sum_{i,m,m'} n_{im\sigma} n_{im'\sigma} - J_h \sum_{i,m,m'} [d^+_{im\uparrow} d^+_{im'\downarrow} d_{im\downarrow} d_{im'\uparrow} + d^+_{im\uparrow} d^+_{im\downarrow} d_{im'\uparrow} d_{im'\downarrow}],$$

where $d_{i,m\sigma}$ is the annihilation operator of an electron of spin σ at site i in orbital m, and $n_{im\sigma} = d^+_{im\sigma} d_{im\sigma}$ is the density operator. Intra- and interorbital repulsions are given by U, $U' = U - 2J_h$, and $U'' = U - 3J_h$, and J_h is the Hund's coupling.

The values of U and J_h are determined on the basis of constrained random-phase approximation (cRPA) calculations that have been performed for the similar material $SrCrO_3$ [21], which gave $U = 2.7$ eV and $J_h = 0.42$ eV. However the lattice parameters of $SrCrO_3$ are smaller with respect to those of $BaCrO_3$ by 0.1 Å so that we expect Cr d orbitals will be more localized in our compound. For this reason we use a slightly larger U keeping the same ratio J_h/U of $SrCrO_3$, namely $U = 3.25$ eV and $J_h = 0.505$ eV. DMFT requires the numerical solution of a quantum impurity model including the local interactions. We use two implementations of DFT+DMFT, one using exact diagonalization (ED) [22,23] and a parallel Arnoldi algorithm [24], the other one using continuous time quantum Monte Carlo (CTQMC) [20,25,26] implementing the conservation laws introduced in Ref. [27]. In order to study phases with magnetic and/or orbital ordering which spontaneously break the translational symmetry of the lattice we introduce a quantum impurity model for each inequivalent chromium site (or sublattice). This is equivalent to assume a local self-energy $\Sigma^{m\sigma}_{ij} = \delta_{ij} \Sigma^{m\sigma}_{ii}$ (i and j being lattice sites), which depends on both the spin (σ) and orbital (m) index, and it is allowed to have a different value on each inequivalent site.

III. RESULTS

A. Paramagnetic solutions without orbital ordering

In the tetragonal unit cell of $BaCrO_3$ [7] ($a = b = 4.09$ Å, $c = 4.07$ Å) the small deviation from a pseudocubic perovskite structure lifts the orbital degeneracy of the t_{2g} orbitals, shifting the xy orbital to lower energy with respect to the degenerate (xz,yz) orbitals. The crystal-field splitting between these orbitals extracted from the PBE band structure is 0.02 eV. Nonmagnetic PBE calculations describe $BaCrO_3$ as a metal, as can be clearly seen from the orbitally-resolved density of states shown in the inset of Fig. 1. All the three bands arising from the t_{2g} orbitals cross the Fermi level and share a similar bandwidth of around 1.7 eV, similarly to the other compound of the same family $SrCrO_3$ [21]. In particular the filling of the chromium bands confirms that the band structure is associated to Cr^{4+} ions and to a total filling of two electrons populating the three

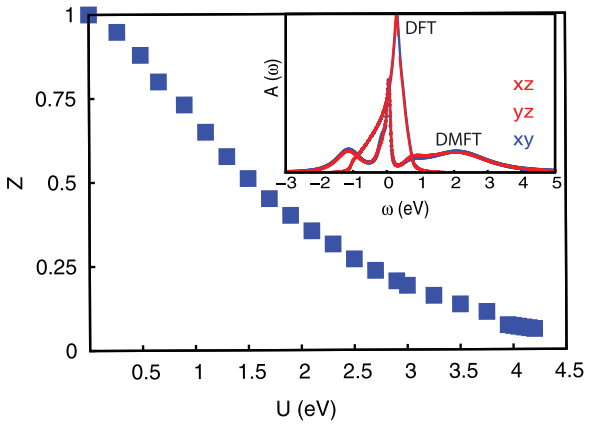

FIG. 1. (Color online) Quasiparticle weight Z as a function of U fixing the ratio J_h/U fixed to the value 0.155 calculated with ED solver. Inset: Resolved orbital density of state of Wannier orbitals (DFT) and DMFT calculations.

t_{2g} orbitals. Since the crystal field splitting is small compared to the bandwidth, the two electrons are equally distributed among the three orbitals, with an orbital population close to 0.66 electrons per orbital.

When we include the interaction effects in DFT+DMFT we expect a reduction of the coherent motion of the carriers, parameterized by an effective quasiparticle bandwidth which may be strongly renormalized with respect to the bare one. The quasiparticle weight Z is a quantitative measure of this effect. A small value of Z is a fingerprint of a strongly correlated state, and a vanishing Z marks a Mott-Hubbard metal-insulator transition. In Fig. 1, we display our results for Z in the paramagnetic state as a function of interaction U, keeping the ratio of J_h/U fixed at the cRPA value 0.155. The near degeneracy of the t_{2g} orbitals makes the quasiparticle weight essentially independent on the orbital index.

The evolution of the quasiparticle weight Z displays the typical Hund's metal behavior, with a clear change of curvature around $U \approx 1.5$ eV, separating a fast drop in the weak-coupling range from a flatter region for intermediate coupling in which Z is small but finite [28]. The Mott phase is indeed reached only at values of U close to 5 eV, significantly larger than the cRPA estimate.

B. Orbital ordering

Our calculations show that pure correlations effect, including the Hund's exchange, do not result in an insulating behavior that is experimentally observed in $BaCrO_3$ [7], and that other physical effects have to be taken into account too. The most natural mechanism to turn a correlated metal into an insulator is some kind of ordering (magnetic, orbital, charge) opening a gap at the Fermi surface.

The most straightforward and common of these mechanisms is a magnetic ordering of the localized spins. This simple scenario seems to be ruled out by local-spin-density-approximation (LSDA) calculations including a Hartree-Fock treatment of interactions (LSDA+U) reported in Ref. [7], where it is stabilized a C-type magnetic structure that however

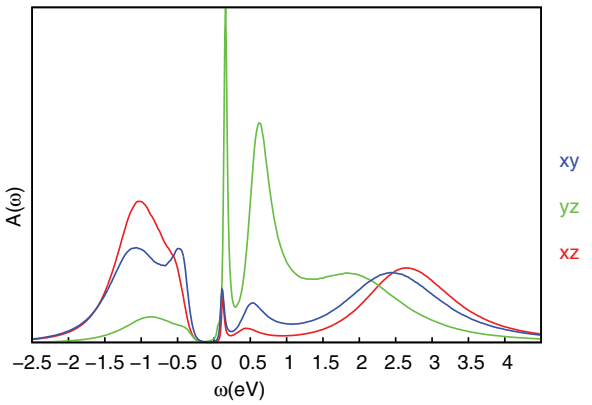

FIG. 2. (Color online) Orbitally-resolved spectral density for $U = 3.5\,\text{eV}$, $J_h = 0.505\,\text{eV}$ in G-type OO for the undistorted tetragonal unit cell of $BaCrO_3$ (results from CTQMC).

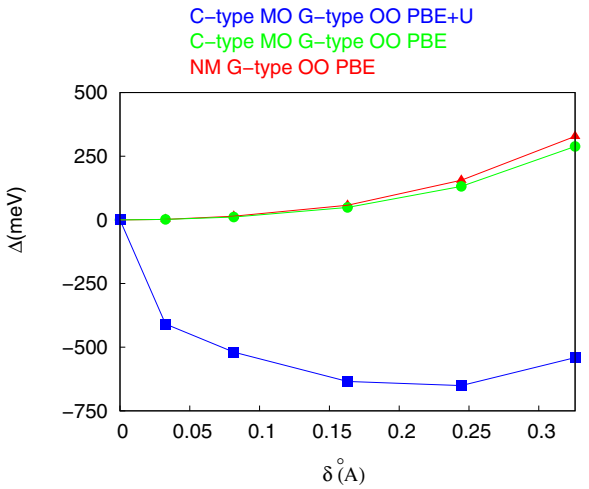

FIG. 3. (Color online) Total energy gain calculated within DFT in the nonmagnetic (NM) and C-type magnetic structure and within DFT+U in the C-type magnetic structure as function of the Jahn-Teller distortion δ (difference between long/short Cr-O bonds).

remains metallic. Our DFT+DMFT calculations confirm that a purely magnetic ordering does not turn the material insulating.

A second possibility is the instability towards orbital ordering. Indeed an orbitally ordered solution with a G-type pattern is found for sizable values of U within DFT+DMFT. On each lattice site we have a nearly filled xy orbital, while xz and yz are alternatively ordered along the three lattice directions. This solution turns out to be the ground state of the system around $U = 3.5\,\text{eV}$, while $U \lesssim 3.25\,\text{eV}$, the ordered state has a slightly larger energy than the orbitally disordered ground state, but it is closely competing. The stable solution for $U = 3.5\,\text{eV}$ is indeed insulating, as shown by the orbitally-resolved spectral density that we report in Fig. 2. This orbital ordering, and the insulating phase may be rationalized in terms of a correlation-driven effective crystal-field splitting that lifts the orbital degeneracy.

C. Jahn-Teller distortions

The tendency towards orbital ordering means that the system is also prone to distortions of the lattice structure as in the case of active Jahn-Teller (JT) effect [29]. In this situation if one allows the ions to relax, they are expected to follow the orbital symmetry exploiting the reduction of the symmetry introduced by strong correlations. It should be noted that a JT-driven splitting competes with the Hund's coupling concerning the orbital occupancies. Whereas the former lifts the degeneracy and tends to populate the lowest-lying orbitals, the latter term favors a more even distribution of the electrons among the orbitals to maximize the total spin and to reduce the overall Coulomb repulsion energy.

The potential role of JT distortions in $BaCrO_3$ and in isoelectronic chromium oxides has not been addressed to our knowledge. However LSDA+U calculations for $CaCrO_3$ predict an orbital ordering in which one electron occupies an orbital with mostly xy character and the second one occupies the two combinations $xz + yz$ and $xz - yz$ in a staggered pattern [12], a configuration that would be further favored by JT distortions. A prominent role of JT distortions is indeed established in $LaVO_3$ and YVO_3, that share the same electronic configuration of $BaCrO_3$ [6,30].

In order to confirm the expectation of a JT distortion in $BaCrO_3$ we perform DFT+U calculations using WIEN2K and an effective interaction $U_{\text{eff}} = U - J = 4\,\text{eV}$ computing the energy as a function of a JT displacement. We assume a staggered JT pattern which mirrors the orbital ordering, in which the octahedra are alternately distorted along the a and b axis. Note that in this framework the interactions refer to atomic orbitals, and therefore the value for the Coulomb interaction is larger than that used for the Wannier orbitals used in DFT+DMFT. In principle the same calculations could have been performed also within DFT+DMFT, but the investigation of structural properties within this approach is extremely heavy from a computational point of view and only a few attempts in this direction have been proposed [31].

In Fig. 3 we show the total energy gain as a function of the JT distortion for the nonmagnetic, C-type magnetic structure within DFT and C-type magnetic structure within DFT+U, which confirm that the presence of a JT instability and the role of the Coulomb interaction in the insulating state of $BaCrO_3$. The energy has a minimum for a finite and quite large value of the distortion only if magnetism is also taken into account. In this situation the system is also insulating. In the following we show how the spontaneous tendency towards orbital ordering in the strongly correlated regime, together with the relaxation of the lattice, explains the insulating state in $BaCrO_3$.

We are now in the position to perform DFT+DMFT calculations for sizeable values of the JT distortion, which we parametrize with a parameter δ which measures the deviation of the Cr-O distances with respect with the undistorted lattice. We considered both G-type and C-type OO as allowed by symmetry considerations, and for the moment we inhibit any magnetic ordering focusing on the paramagnetic orbitally-ordered solution. The results weakly depend on the value of δ, and we present calculations for $\delta = 0.17$ Å, which is a reasonable value for $BaCrO_3$ in view of the above results.

The distortion of the oxygen sites splits the position of the energy levels of the (xy,xz,yz) orbitals: At a particular Cr site

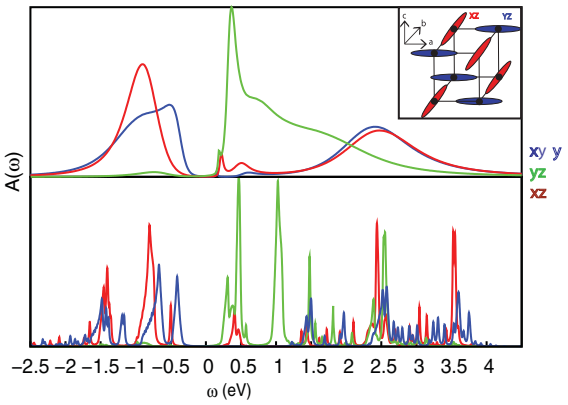

FIG. 4. (Color online) Resolved orbital spectral density for $U = 3.25\,\text{eV}$, $J_h = 0.505\,\text{eV}$ in G-type OO for $\delta = 0.17$Å. Lower panel shows results using the ED solver, the upper panel results from CTQMC. Inset: Orbital arrangement (G-type OO) in the plane of tetragonal unit cell with the two inequivalent Cr-O distances.

the xy lies between xz and yz orbitals which are higher and lower in energy by an amount of 0.05 eV for a distortion $\delta = 0.17$ Å. The noninteracting (DFT) orbital-resolved density of states shows three bands with nearly the same bandwidth and shape of 1.8 eV with orbital occupancies being 0.79, 0.66, and 0.55 from the lower to higher energy level (xz,xy,yz), respectively, on a lattice site where xz is the lowest-lying level. Obviously, in the OO phase, the occupancies of the xz and yz orbitals alternate in the a-b plane. The above results are essentially independent on the choice of C-type or G-type orbital ordering.

In this lattice configuration the introduction of strong correlations via DFT+DMFT enhance the occupancies of xz and xy orbitals with respect to yz as if the crystal-field splitting is effectively increased. Interestingly, the effect is realized via a strongly frequency-dependent real part of the self energy.

In the relevant case of $U = 3.25\,\text{eV}$ and $J_h = 0.505\,\text{eV}$ the orbital occupancies of t_{2g} orbitals in the insulating solutions are 0.96, 1.0, and 0.04 for xz,xy,yz respectively (on the sublattice where xz is favored with respect to yz), showing that correlations enhance the orbital correlations and result in almost perfect orbital ordering. The orbital-resolved spectral density with the chosen values of U and J_h in Fig. 4 show that with the inclusion of a JT distortion the material is correctly found to be an insulator with a gap in good agreement with experimental values [7].

D. Magnetic ordering

The relative orientation of orbitals on neighboring cations then determines the superexchange interactions between the unpaired d electrons, which in turn determine the magnetic ordering patterns. The presence of a JT distortion is expected to give rise to a strong interplay between orbitals and spins [32,33]. Indeed the antiferro-orbital alternation of xz and yz orbitals along each of the a,b,c of the crystal structure determines a ferromagnetic coupling which competes with the antiferromagnetic coupling of the ferro-orbital ordered xy orbitals in ab plane and ferromagnetic coupling along c direction. Therefore we performed calculations for different orbital- and spin-ordering patterns to determine the outcome of the above competition.

For perovskites with partially occupied e_g orbitals, such as cuprates [34] and manganites [35] or other Cr based compounds [36], the JT energy greatly exceeds the superexchange coupling between unpaired electrons, so that orbital and magnetic ordering temperatures are well separated. In the case of $BaCrO_3$, where only t_{2g} orbitals contribute to low-energy physics, we expect a weaker JT coupling and orbital and magnetic transitions could occur in the same temperature range. The orbital and spin orderings in $BaCrO_3$ might develop the same temperature-induced magnetization reversal [37] and different ordering temperatures [6] as in YVO_3 single crystal.

The calculated orbital occupancies establish that the lattice distortion triggers the magnetic ordering with a C-type (each spin is antiparallel to all others in the ab plane but parallel along the c axis) or G-type (every spin is antiparallel to all its neighbors) magnetic structure stabilized depending if a G-type/C-type OO is considered as expected from the Goodenough-Kanamori rule for superexchange [33]. In the magnetically ordered states the (xz,xy,yz) orbitals are filled by 0.95(0.0), 0.98(0.02), 0.03(0.02) electrons in the majority(minority) channels, respectively. Once again, these populations do not depend on the precise nature of the ordered state. Magnetic ordering further increases the value of the gap by 0.1 eV as can be seen form the resolved orbital spectral density in Fig. 5 for the case of C-type magnetism and G-type OO.

We mention here that within DFT+DMFT we discard the possibility of a octahedral tilting with a $GdFeO_3$ type of distortion as in the case of $CaCrO_3$ crystal structure being the ionic radius of Ba larger as for Sr. Moreover a combination of JT distortions and tilting of the oxygen octahedra allows by

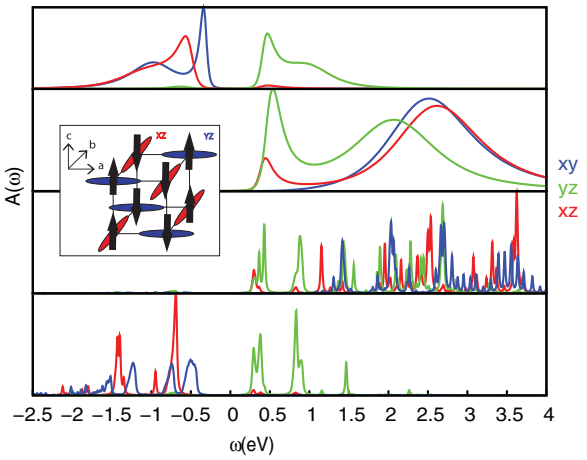

FIG. 5. (Color online) Orbitally-resolved spectral density for $U = 3.25\,\text{eV}$, $J_h = 0.505\,\text{eV}$ in G-type orbital ordering and C-type spin ordering for $\delta = 0.17$ Å. Lower two panels: Results using the ED solver for majority/minority spin channels. Upper two panels: Results from CTQMC for majority/minority spin channels. Inset: Spin (C-type AFM) and orbital (G-type OO) arrangement in the plane of tetragonal unit cell with the two inequivalent Cr-O distances.

symmetry for many different space groups going beyond the scope of this paper.

IV. CONCLUSIONS

In conclusion, we use a DFT+DMFT approach to study the electronic properties of the recently synthesized compound $BaCrO_3$, which is a nontrivial insulator. We show that $BaCrO_3$, in its tetragonal crystal structure, would be a strongly correlated metal in which the degree of electronic correlations is tuned by the Hund's coupling. We reveal $BaCrO_3$ to be close to an orbital ordered state driven by the effect of electronic interactions, which lower the electronic symmetry of the tetragonal symmetry. We predict that the insulating character arises from the combination of the above correlation effects and a Jahn-Teller splitting of the t_{2g} orbitals, which leads to orbital ordering and to a gap in good agreement with the experimental value. Magnetic ordering compatible with the Goodenough-Kanamori rule establishes in the JT distorted insulating state. Experimental investigations of the crystal structure of $BaCrO_3$ would be a direct test of our scenario.

After submission of the paper, we became aware of a related work by Jin *et al.*, Ref. [38], in which on the basis of relativistic DFT+U calculations a orbital ordering has been found, induced by strain in $BaCrO_3$. We repeated our calculations within DFT+U for the experimental tetragonal structure without strain including the relativistic effect of spin-orbit coupling. We again found our proposed magnetic and orbital ordering to be the most stable ground state configuration, with only a very tiny effect of the spin-orbit coupling on the electronic structure of $BaCrO_3$.

ACKNOWLEDGMENTS

We wholeheartedly thank S. Streltsov and L. de' Medici for precious discussions. G.G. and M.C. acknowledge financial support by the European Research Council under FP7/ERC Starting Independent Research Grant "SUPERBAD" (Grant Agreement No. 240524). M.A. acknowledges support from the Austrian Science Fund (FWF) through the SFB VICOM, subproject F04103. Calculations have been performed on the TU Graz *dcluster* and at CINECA (HPC project lsB06_SUPMOT).

[1] A. Georges, L. De' Medici, J. Mravlje, Annu. Rev. Condens. Matter Phys. **4**, 137 (2013).
[2] K. Haule and G. Kotliar, New J. Phys. **11**, 025021 (2009).
[3] J. Mravlje, M. Aichhorn, T. Miyake, K. Haule, G. Kotliar, and A. Georges, Phys. Rev. Lett. **106**, 096401 (2011).
[4] L. de' Medici, S. R. Hassan, M. Capone, and Xi Dai, Phys. Rev. Lett. **102**, 126401 (2009).
[5] L. de' Medici, G. Giovannetti, and M. Capone, Phys. Rev. Lett. **112**, 177001 (2014).
[6] G. R. Blake, T. T. M. Palstra, Y. Ren, A. A. Nugroho, and A. A. Menovsky, Phys. Rev. Lett. **87**, 245501 (2001).
[7] Z. H. Zhu, F. J. Rueckert, J. I. Budnick, W. A. Hines, M. Jain, H. Zhang, and B. O. Wells, Phys. Rev. B **87**, 195129 (2013).
[8] J.-S. Zhou, C. Q. Jin, Y. W. Long, L. X. Yang, and J. B. Goodenough, Phys. Rev. Lett. **96**, 046408 (2006).
[9] B. L. Chamberland, Solid State Commun. **5**, 663 (1967).
[10] A. J. Williams, A. Gillies, J. P. Attfield, G. Heymann, H. Huppertz, M. J. Martinez-Lope, and J. A. Alonso, Phys. Rev. B **73**, 104409 (2006).
[11] A. C. Komarek, T. Möller, M. Isobe, Y. Drees, H. Ulbrich, M. Azuma, M. T. Fernandez-Diaz, A. Senyshyn, M. Hoelzel, G. André, Y. Ueda, M. Grüninger, and M. Braden, Phys. Rev. B **84**, 125114 (2011).
[12] S. V. Streltsov, M. A. Korotin, V. I. Anisimov, and D. I. Khomskii, Phys. Rev. B **78**, 054425 (2008).
[13] K. W. Lee and W. E. Pickett, Phys. Rev. B **80**, 125133 (2009).
[14] P. Hohenberg and W. Hohn, Phys. Rev. **136**, B864 (1964); W. Kohn and L. J. Sham, *ibid.* **140**, A1133 (1965).
[15] A. Georges, G. Kotliar, W. Krauth, and M. J. Rozenberg, Rev. Mod. Phys. **68**, 13 (1996).
[16] J. P. Perdew, K. Burke, and M. Ernzerhof, Phys. Rev. Lett. **77**, 3865 (1996).
[17] P. Giannozzi, S. Baroni, N. Bonini, M. Calandra, R. Car, C. Cavazzoni, D. Ceresoli, G. L. Chiarotti, M. Cococcioni, I. Dabo, A. Dal Corso, S. Fabris, G. Fratesi, S. de Gironcoli, R. Gebauer, U. Gerstmann, C. Gougoussis, A. Kokalj, M. Lazzeri, L. Martin-Samos, N. Marzari, F. Mauri, R. Mazzarello, S. Paolini, A. Pasquarello, L. Paulatto, C. Sbraccia, S. Scandolo, G. Sclauzero, A. P. Seitsonen, A. Smogunov, P. Umari, and R. M. Wentzcovitch, J. Phys. Condens. Matter **21**, 395502 (2009).
[18] P. Blaha, K. Schwarz, P. Sorantin, and S. B. Trickey, Comput. Phys. Commun. **59**, 399 (1990); K. Schwarz and P. Blaha, Comput. Mater. Sci. **28**, 259 (2003).
[19] A. A. Mostofi, J. R. Yates, Y.-S. Lee, I. Souza, D. Vanderbilt, and N. Marzari, Comput. Phys. Commun. **178**, 685 (2008).
[20] M. Ferrero and O. Parcollet, TRIQS: a Toolbox for Research in Interacting Quantum Systems, http://ipht.cea.fr/triqs.
[21] Loig Vaugier, Hong Jiang, and Silke Biermann, Phys. Rev. B **86**, 165105 (2012).
[22] M. Caffarel and W. Krauth, Phys. Rev. Lett. **72**, 1545 (1994).
[23] M. Capone, L. de' Medici, and A. Georges, Phys. Rev. B **76**, 245116 (2007).
[24] R. B. Lehoucq, D. C. Sorensen, and C. Yang, *ARPACK Users Guide* (SIAM, Philadelphia, 1997).
[25] E. Gull, A. J. Millis, A. I. Lichtenstein, A. N. Rubtsov, M. Troyer, and P. Werner, Rev. Mod. Phys. **83**, 349 (2011).
[26] L. Boehnke, H. Hafermann, M. Ferrero, F. Lechermann, and O. Parcollet, Phys. Rev. B **84**, 075145 (2011).
[27] N. Parragh, A. Toschi, K. Held, and G. Sangiovanni, Phys. Rev. B **86**, 155158 (2012).
[28] L. de' Medici, J. Mravlje, and A. Georges, Phys. Rev. Lett. **107**, 256401 (2011).
[29] H. A. Jahn and E. Teller, Proc. R. Soc. A **161**, 220 (1937).
[30] Zhong Fang and Naoto Nagaosa, Phys. Rev. Lett. **93**, 176404 (2004).
[31] I. Leonov, N. Binggeli, Dm. Korotin, V. I. Anisimov, N. Stojic, and D. Vollhardt, Phys. Rev. Lett. **101**, 096405 (2008).

[32] K. I. Kugel and D. I. Khomskii, Sov. Phys. Usp. **25**, 231 (1982).
[33] J. B. Goodenough, *Magnetism and Chemical Bond* (Interscience, New York, 1963).
[34] L. Paolasini, R. Caciuffo, A. Sollier, P. Ghigna, and M. Altarelli, Phys. Rev. Lett. **88**, 106403 (2002).
[35] J. Rodriguez-Carvajal, M. Hennion, F. Moussa, A. H. Moudden, L. Pinsard, and A. Revcolevschi, Phys. Rev. B **57**, R3189 (1998).
[36] S. Margadonna and G. Karotsis, J. Mater. Chem. **17**, 2013 (2007); G. Giovannetti, S. Margadonna, and J. van den Brink, Phys. Rev. B **77**, 075113 (2008).
[37] Y. Ren, T. T. M. Palstra, D. I. Khomskii, E. Pellegrin, A. A. Nugroho, A. A. Menovsky, and G. A. Sawatzky, Nature **396**, 441 (1998).
[38] Hyo-Sun Jin, Kyo-Hoon Ahn, Myung-Chul Jung, and K.-W. Lee, Phys. Rev. B **90**, 205124 (2014).